MICROSTRUCTURAL, THERMAL, MAGNETIC AND DIELECTRIC PROPERTIES OF COBALT DOPED BARIUM CALCUM HEXAFERRITE PREPARED BY A SOL-GEL ROUTE

Chauhan C.C[a], Jotania R. B[b*]

Address for Correspondence

[a] Department of Physics, Institute of Technology, Nirma University, Ahmedabad, 382481, Gujarat, India.
[b] Department of Physics, University School of Sciences, Gujarat University, Ahmedabad, 382481,Gujarat, India

ABSTRACT

A series of w-type hexagonal ferrites with the composition $BaCo_xCa_{2-x}Fe_{16}O_{27}$ (x = 0.4, 0.8, 1.2, 1.6, 1.8 and 2.0) were synthesized using a Stearic acid gel route with and without presence of Cetyletrimethyle ammonium bromide. The precursors were calcinated at 950ºC for 4 hrs in a furnace and then slowly cooled to room temperature in order to obtained $BaCo_xCa_{2-x}Fe_{16}O_{27}$ crystalline ferrite powder. The effect of cationic surfactant Cetyletrimethyle ammonium bromide (CTAB) on structural and thermal properties were studied. The structural properties of the samples were studied by using XRD, FTIR and SEM. Decomposition behavior is investigated by means of thermal analysis (TGA). Thermo gravimetric analysis confirms the high thermal stability of w-type hexagonal ferrite particles synthesized in presence of CTAB. The field dependent magnetic properties of prepared Ba-Ca hexaferrite particles were investigated at room temperature by using Vibrating Sample Magnetometer (VSM). The maximum coercivity and saturation magnetization of prepared w-type hexaferrite samples were determined by a VSM. The value of saturation magnetization depends on amount of cobalt substitution. The sample (x = 0.8) shows high saturation magnetisation (~71 emu/g), where as the sample (x = 2.0) exhibits low saturation magnetisation (~65 emu/g). Magnetic study reveals that prepared $BaCo_xCa_{2-x}Fe_{16}O_{27}$ (x = 1.8 and 2.0) hexaferrite particles prepared in presence of CTAB possess single magnetic domain.The dielectric measurements were carried out at room temperature between the frequency range 100 Hz to 1 MHz.

KEYWORDS W-type cobalt doped Ba-Ca hexaferrite, Stearic acid gel route, surfactant, structural properties, magnetic properties.

INTRODUCTION

Barium hexaferrite is a ferromagnetic material with high performance of permanent magnetic property, high uniaxial magnetocrystallilne anisotropy constant, saturation magnetization, excellent chemical stability and corrosion resistance [1,2]. Recently, ceramic materials are classified by their high resistivity and high permeability, so a numerous products of them are used in industry, technology, electronic devices, communication equipments, high density magnetic recording media, materials for permanent magnets and microwave devices [3-8]. The interest to study hexaferrites comes from their specific magnetic behavior and electrical conduction [9,10].

The crystal structure of w-type hexagonal ferrite is very complex and can be considered as a superposition of R and S blocks along the hexagonal C-axis with a structure of RSSR*S*S*, where R is a three-oxygen-layer block with composition $BaFe_6O_{11}$, S (spinel block) is a two-oxygen layer block with composition Fe_6O_8 and '*' means that the respective block is turned $180°$ around the hexagonal axis. The application of hexaferrite in high density magnetic recording media require materials with high control of homogeneity, morphology and magnetic properties resulting from their methods of preparation and heat treatments [11, 12].

The conventional ceramic method for preparation of Ba hexaferrite is the solid state reaction between $BaCO_3$ and Fe_2O_3 at high calcining temperature (~1200°C), which has inherent disadvantages such as chemical inhomogeneity, coarse grain size and then need to milling to get submicron sizes, which in turn leads to entrance of impurities and inducing lattice strains during the milling. To avoid this various methods like the sol-gel [13], the chemical co-precipitation [14,15], hydrothermal synthesis [16,17], micro emulsion and reverse micelle [18,19] and the orgo metallic precursor synthesis [20]. We have adopted stearic acid sol gel method to synthesize w-type $BaCa_{2-x}Co_xFe_{16}O_{27}$ (x = 0.4, 0.8, 1.2, 1.6, 1.8 and 2.0) hexaferrite particles.

In the present paper, we report the microstructural, thermal, magnetic and dielectric properties of $BaCa_{2-x}Co_xFe_{16}O_{27}$ hexaferrite particles synthesized by a sol gel route with and without the presence of surfactant, Cetyle trimethyl ammonium bromide (CTAB). The effect of surfactants on magnetic and dielectric properties of $BaCa_{2-x}Co_xFe_{16}O_{27}$ has been studied.

EXPERIMETAL PROCEDURE

A.R. Grade barium hydroxide $(Ba(OH)_2)$, ferric nitrate $(Fe(NO_3)_2.9H_2O)$, cetyltrimethyl ammonium bromide (CTAB), cobalt acetate and calcium nitrate $(Ca(NO_3)_2).4H_2O$ were used as starting materials. Iron nitrate $(Fe(NO_3)_2).9H_2O$, Sigma Aldrich, of A.R grade were used. Samples with composition $BaCa_{2-x}Co_xFe_{16}O_{27}$ were prepared using a stearic acid sol–gel method. The stoichiometric amounts of iron nitrate $(Fe(NO_3)_2).9H_2O$, barium hydroxide $(Ba(OH)_2)$, calcium nitrate $(Ca(NO_3)_2).4H_2O$ and cobalt acetate were mixed in an appropriate amount of a stearic acid solution. The mixture was heated at 80–100°C for 2 hr under stirring and then cooled to room temperature. The gel precursor so formed was decomposed at 500°C for 1 hr and subsequently calcinated at 650, 750, 850, 950 and 1050°C for 4 h in air and slowly cooled in furnace to obtain a $BaCa_{2-x}Co_xFe_{16}O_{27}$ (x = 0.4, 0.8, 1.2, 1.6 and 2.0) hexaferrite powder. The same procedure was repeated using surfactant CTAB.

RESULTS AND DISCUSSION

1. Structural Investigation and Phase Analysis:

The X-ray diffraction patterns for the system $BaCa_{2-x}Co_xFe_{16}O_{27}$ gel and calcinated samples (x = 0.4, 0.8, 1.2, 1.6 and 2.0) were recorded on Philips diffractometer (PW 1830) using CuKα radiation (λ = 1.5405 Å) with a step scan of 0.02˚C/min. Figure 1 shows the XRD patterns of normal $BaCa_{2-x}Co_{0x}Fe_{16}O_{27}$ hexaferrite (x = 0.4, 0.8, 1.2, 1.6 and 2.0).

The position and intensity of X-ray diffraction lines for BaW are given in Fig. 1, based on JCPDS-International Centre for Diffraction Data (Card no.78-0135). The XRD pattern shows three phases (W, M and α-Fe$_2$O$_3$ phase). It was reported [20] that the unit cell of w-type phase is closely related to M-phase; the only difference is that the successive R blocks are inter placed by two S-blocks instead of one as in the M-phase. It was also mentioned by Lotgering [21] that W-type hexagonal ferrite is chemically unstable; some of w-phase gets decomposed to M and α-Fe$_2$O$_3$ phase [21,22].
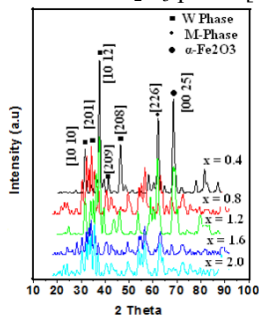

Figure 1 X-ray diffraction patterns for powders of BaCa$_{2-x}$Co$_x$Fe$_{16}$O$_{27}$ (x = 0.4, 0.8, 1.2, 1.6, 2.0) samples calcinated at 950°C.

Lattice constants a and c of hexagonal barium ferrite were calculated using Eq. (1):

$$\frac{1}{d} = \frac{4}{3}\frac{h^2 + k^2 + l^2}{a^2} + \frac{l^2}{c^2} \quad (1)$$

where h, k and l are Miller indices, d is inter planer distance. Lattice volume of all the samples can be obtained using Eq. (2):

$$V = \frac{\sqrt{3}}{2}a^2 c \quad (2)$$

The lattice parameters a and c and the variation of lattice parameter and their ratio c/a with co^{+2} (0.65 Å) substitution are given in figure 2 and Table 1. It is seen that lattice parameters a and c decreases linearly from 0.593 to 0.587 nm, and from 3.323 to 3.278 nm, respectively, as BaCa$_{1.6}$Co$_{0.4}$Fe$_{16}$O$_{27}$ is changed to BaCo$_2$Fe$_{16}$O$_{27}$. This is due to relatively small ionic radius of Co^{+2} (0.65 Å) as compared with that of Ca^{+2} (0.99 Å). As a result, the cell volume of barium ferrite, V, decreases with the substitution of Co^{+2}. The values of calculated lattice parameter are in the same range as in the literature: a = 5.88 Å, c = 32.84 Å and c/a = 5.88 for BaCa$_{2-x}$Co$_x$Fe$_{16}$O$_{27}$ [23].

Table 1: Lattice constant a, c, volume of unit cell (V) and x-ray density for BaCa$_{2-x}$Co$_x$Fe$_{16}$O$_{27}$

Concentration x	Lattice Parameter a (nm)	Lattice Parameter c (nm)	c/a	Volume V(nm^3)
0.4	0.593	3.323	5.603	2.024
0.8	0.592	3.298	5.571	2.002
1.2	0.590	3.292	5.580	1.985
1.6	0.589	3.285	5.577	1.974
2.0	0.587	3.278	5.584	1.956

Table 2. Room temperature Magnetic parameters of BaCa$_{2-x}$Co$_x$Fe$_{16}$O$_2$ hexaferrite powder prepared by a stearic acid gel route (Coercivity- Hc, Saturation Magnetization- Ms, remanent Magnetization- Mr and Magnetocrystalline anisotropy constant K measured at 15 kOe).

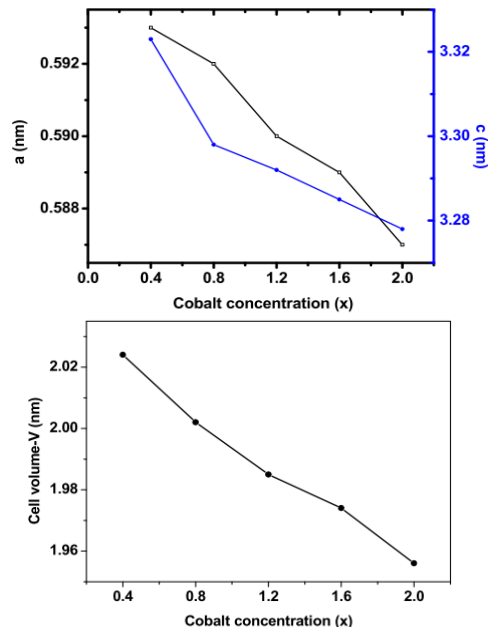| x	Ms [emu/gm]	Mr [emu/gm]	Hc [Oe]	Mr/Ms	K [HA^2/Kg]
0.4	1.342	0.633	1130	0.471	9.52 x 10^{-4}
0.8	1.62	0.76	625	0.469	6358.5 x 10^{-7}
1.2	1.04	0.412	750	0.396	4898.4 x 10^{-7}
1.6	0.96	0.507	1750	0.5281	10550 x 10^{-7}
2.0	0.475	0.2753	2500	0.5795	7457.5 x 10^{-7}

Figure 2 The dependence of lattice parameters, a and c, as well as cell volume V on cobalt concentration x for BaCa$_{2-x}$Co$_x$Fe$_{16}$O$_{27}$ (x = 0.4, 0.8, 1.2, 1.6 and 2.0) hexaferrite samples

2. FTIR Analysis:

To investigate ferrite phase formation the room temperature Fourier transform infrared spectra (FTIR) of BaCa$_{2-x}$Co$_x$Fe$_{16}$O$_{27}$ powders were recorded at room temperature in wave number range from 4000 cm^{-1} to 400 cm^{-1} by using the KBr pallet method on FTIR Bruker Tensor 27 model. The FTIR spectra of the powder calcinated at 950°C (Figure 3) and for various concentration (x = 0.4, 0.8, 1.2, 1.6 and 2.0) shows the absorption band at ~3340 cm^{-1} which is due to H$_2$O and OH^{-1} vibrations. This bands may be due to the moisture present in the powder. No NO$_3^{-1}$ absorption bands are found in spectra, indicating the sample without any organic or inorganic impurity. The absorption band between 590 cm^{-1} to 440 cm^{-1} confirms the ferrite phase formation [24,25].
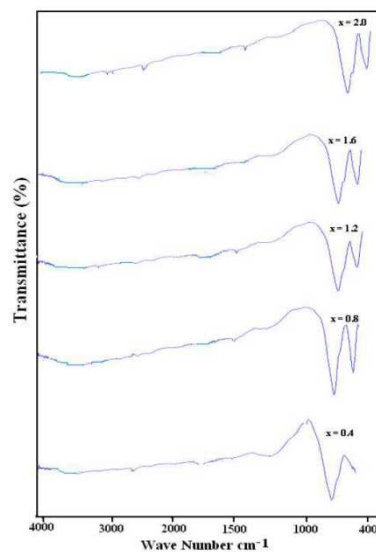

Figure 3 FTIR spectra of normal BaCa$_{2-x}$Co$_x$Fe$_{16}$O$_{27}$ (x = 0.4, 0.8, 1.2, 1.6, 2.0) samples calcinated at 950°C.

3. Thermal Studies:

TGA curves of dried materials were recorded using a SII Differential Thermal analyzer Model No.SSC 5100 in the region of 40°C to 700°C with a rate of 10°C/min. During the heat treatment of gel, several processes such as dehydration, oxidation of the

residual organic groups, decomposition and sintering take place. The TGA curves (Figure 4a and 4b) of $BaCa_{1.2}Co_{0.8}Fe_{16}O_{27}$ dried gels (normal and with surfactant) shows the three steps of weight loss. The first step of weight loss below 200˚C is ~7% due to evaporation of water for both the samples. The second step of weight loss occurs between 100˚C and 200˚C, ~28% for normal gel and ~27% for the gel in presence of surfactant. The third step of weight loss between 200˚C and 300˚C is ~ 3% for both the samples due to decomposition of organic substances. Then after for the normal gel there is less weight loss for the normal sample and almost no weight loss for the gel prepared in presence of surfactant, increasing the stability of the sample.
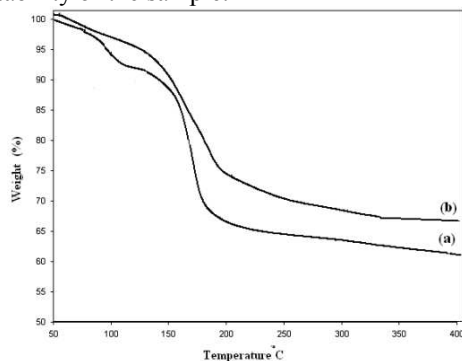

Figure 4 TGA curve of $BaCa_{1.2}Co_{0.8}Fe_{16}O_{27}$ (a) normal gel and (b) with CTAB.

4. Microstructural Analysis:

Scanning electron micrographs of prepared Ba-Mg hexaferrite samples are obtained using a Make-Leo/Lica model Stereo scan 440 scanning electron microscope. The SEM micrographs of $BaCa_{2-x}Co_xFe_{16}O_{27}$ hexaferrite powder shows (Figure 5 and 6) the agglomerated and nonuniform particle in absence of surfactant, whereas in presence of surfactant the separated and uniform particles of 200nm is obtained. The attractive force acting between the molecules of barium and ferric ions might be the result of surface in homogeneity in the sample. Addition of surfactant CTAB controls the particle shape and size.
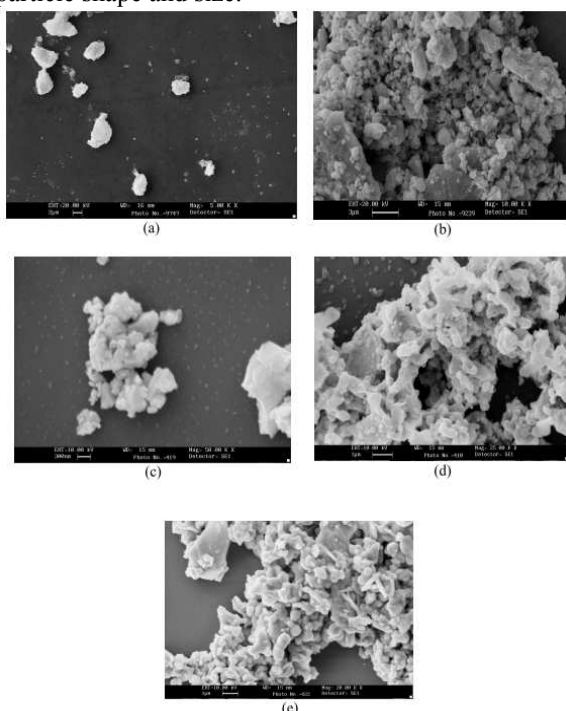

Figure 5 SEM images of $BaCa_{2-x}Co_xFe_{16}O_{27}$ hexaferrites without surfactant (a) x = 0.4, (b) x = 0.8,

(c) x = 1.2, (d) x = 1.6 and (e) x = 2.0 calcinated at 950°C for 4 hours.

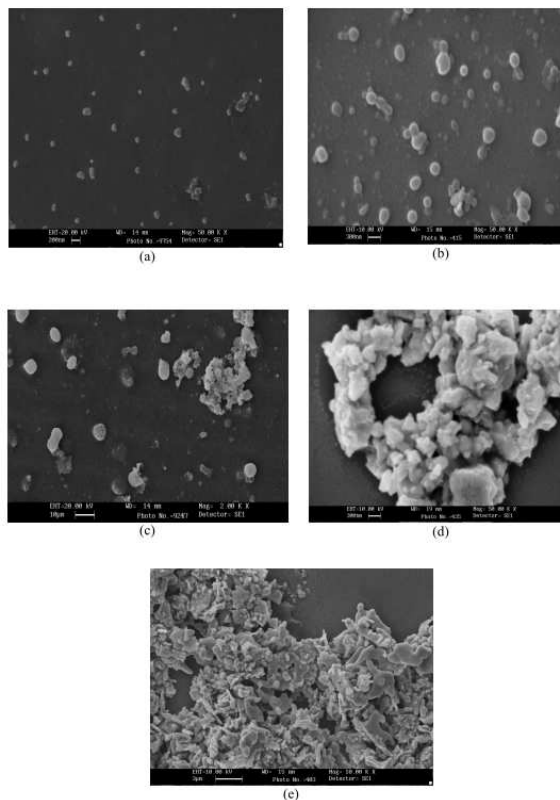**Figure 6 SEM images of $BaCa_{2-x}Co_xFe_{16}O_{27}$ hexaferrites prepared in presence of CTAB surfactant, (a) x = 0.4, (b) x = 0.8, (c) x = 1.2, (d) x = 1.6 and (e) x = 2.0 calcinated at 950°C for 4 hours.**

5. Magnetic Properties:

The magnetization curves and M-H loop of Ba-Ca hexaferrite particles was recorded at room temperature using VSM, EG & G Princeton Applied Research instrument Model 4500 under the applied field of 15 KOe. The hysteresis loops of the samples are shown in figure 7. The magnetic parameters are listed in Table 2. The saturation magnetization Ms of $BaCa_{2-x}Co_xFe_{16}O_{27}$ decreases from x = 0.4 to 2.0. The saturation magnetization Ms, as a function of x is plotted with the increase in cobalt substitution (Figure 8). Ms is found to increase first, reach a smooth maximum value at x = 0.8, and then decreases. This behaviour can be explained as:

The non magnetic Co^{+2} ions prefer the tetrahedral site with spin down. Therefore Ca^{+2} ions occupying these sites decrease the negative magnetization, and thus leading to an increase in the total magnetization. On the other hand, Co^{+2} ions prefer to occupy the octahedral site. This can lead to increase or decrease in the net magnetization respectively. As the substitution of cobalt increases coercivity increases upto x = 1.2 and from x = 1.6 the coercivity decreases. The values of Mr/Ms for all the samples are about 0.5, indicating that $BaCa_{2-x}Co_xFe_{16}O_{27}$ powder of single magnetic domains was produced [26].The coercivity of particles is determined [27] by using magnetocrystalline anisotropy constant K and saturation magnetization.

$$H_c = \frac{2K}{\mu_0 M_s} \qquad (3)$$

where, μ_0 is the universal constant of permeability in free space equal to $4\pi \times 10^{-7}$ H/m. Magnetocrystalline anisotropy constant K can be calculated from Eq. 1. According to ref. [28], the energy barrier (EA) for

rotation of magnetization orientation in a single domain particle is given by

$$E_A = KV_p \sin^2\theta \qquad (4)$$

where V_p is the volume of the particle and θ is the angle between an applied field and the easy axis of the particle. The energy barrier (E_A) is proportional to the product of KV_p, under the same magnetization direction. Using Eq. 4 one can estimate the order of energy barrier for all the samples that follow the order $E_{A1} < E_{A2} < E_{A4} < E_{A5} < E_{A3}$.

The coercivity is considered as measure of the magnetic field strength necessary to achieve changes of the magnetization direction of material, low value of anisotropy of the material will give low activation energy barrier (observed in the sample with concentration x = 1.2), and hence low applied field will be required for reversing the spin and hence low coercivity.
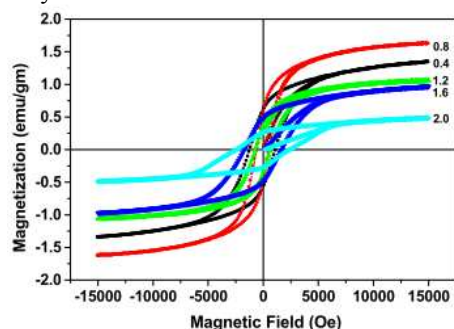

Figure 7 Hysteresis loop of BaCa$_{2-x}$Co$_x$Fe$_{16}$O$_{27}$ with (a) x = 0.4, (b) x = 0.8, (c) x = 1.2, (d) x = 1.6 and (e) x = 2.0 calcinated at 950°C.

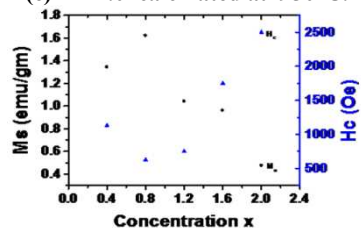**Figure 8 Variation of Saturation magnetization (Ms) and coercivity (Hc) with Cobalt concentration (x)**

6. Dielectric measurements:

The dielectric measurements were carried out at room temperature using Hewlett-Packard 4284 LCR meter between the frequency range 100 Hz to 1MHz. Figure 9a shows that there is a traditional dispersion of dielectric constant with increasing frequency. This behaviour of a dielectric may be explained quantitatively by the supposition that the mechanism of the polarization process in hexaferrite system is similar to that of the conduction process. The electrical conduction mechanism can be explained by the electronic hopping model of Heikes and Johnson [29]

$$(Fe^{2+} \leftrightarrow Fe^{3+} + e \text{ or } Ca^{2+} \leftrightarrow Ca^{3+} + e) \qquad (5)$$
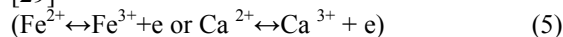
The polarization decreases with increasing frequency and reaches constant value when the hopping frequency of electrons between Fe^{+2} Fe^{+3} ions cannot follow any more fast changes of alternating field. It is known that effect of polarization is to reduce the field inside the medium. Therefore the dielectric constant of the substance may be decreases substantially as the frequency is increase. The behaviour of tanδ with frequency (Figure 9b) is showing the expected decrease of tan δ with increasing frequency. The value of loss tangent obtained in present work is very small at frequencies from a few KHz to about MHz, which is much lower than that of the conventional

ceramic method [30-32]. The dielectric loss arises, if polarization lags behind the applied altering field and caused by the structural in homogeneties. The low dielectric loss obtained in the present work is therefore attributed to more structurally perfect and homogenous hexaferrites processed by stearic acid gel route. The decrease in dielectric loss tangent with increase in frequency is in accordance with the Koop's phenomenological model [31].The dielectric loss decreases substantially with increasing frequency and reaches a constant value later on [32-34]. This is exactly with the fact that at lower frequencies, the resistivity is high and the grain boundaries effect is dominant. Thus more energy is required for electron interchange between Fe^{+2} and Fe^{+3} ions, located at grain boundaries and thus dielectric constant manifested a high value. At higher frequencies, when the resistivity is low and the grain influence is dominant, low energy is needed for hopping process between Fe ions located in the grains, and as a result dielectric loss possess low values. The maximum value of dielectric loss is observed when the hopping frequency is equal to the frequency of the applied field.
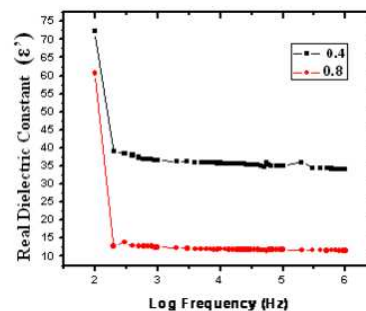

Figure 9a Real Dielectric constant (ε') over frequency of BaCa$_{2-x}$Co$_x$Fe$_{16}$O$_{27}$ (x=0.4, 0.8) hexaferrites calcinated at 950°C for 4 hours.
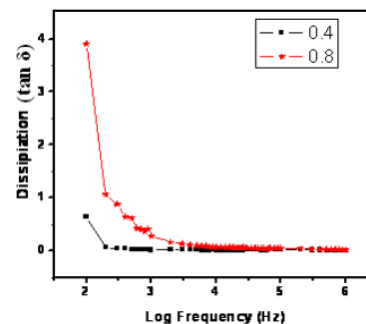
Figure 9b Loss tangent (tan δ) over frequency of BaCa$_{2-x}$Co$_x$Fe$_{16}$O$_{27}$ (x=0.4, 0.8) hexaferrites calcinated at 950°C for 4 hours.

CONCLUSIONS

The observation from Thermal, VSM and dielectric studies can be summarized as follows:

1. A cobalt substituted barium calcium hexaferrite powder is synthesized using a stearic acid gel method without and in presence of cationic surfactant CTAB.
2. Addition of surfactant CTAB increases the thermal stability of the sample.
3. Low coercivity is observed for the sample with concentration x = 1.2.
4. The decrease in dielectric constant with increase in frequency is explained in the terms of supposition that the mechanism of electric polarization takes place.
5. The decrease in dielectric loss tangent with increase in frequency experimentally agree with Koop's model.

6. ACKNOWLEDGEMENT

REFRENCES

1. R.C. Pullaar, A.K. Bhattacharya, Mater. Lett. 57(2002)537.
2. J. Dho J, E.K. Lee, J.Y. Park, N.H. Hur, J. Magn. Magn. Mater. 285(2005)164.
3. B. Vishwanatha, V.R.K. Murthy, Ferrite Materials; Science and Technology, Narosa publishing house, New Delhi, U.P. 1990, pp. 429.
4. E.C. Snelling, Soft Ferrites/Properties and Appllication; second ed. Butter worths, London, 1988, pp.1.
5. J. Smith, H.P.J. Wijn, Ferrites, Philips Technical Library, Eindhoven, 1959, pp. 195.
6. A. Morisako, M. Matsumoto, M. Naoe, IEEE Trans. Magn. M. 3024 (1988)24.
7. T. L. Hylton, M. A. Parker, M. Ullah, K. R. Coffey, R. Umphress, J. K. Haward, J. Appl. Phys. 75(1994)5960.
8. T.P. Niesen, M.R. de Guire, J. Electroceram. M. 169 (2001)6.
9. H. Gractsh, F. Haberey, R. Leckebusch, M. Rosenberg, K. Sahl, IEEE Trans. Magn. Magn. 495 (1984)20.
10. M.N. Deschizeux, M Regi, J.C. Joubert, J. Solid State Chem. J. C. 234(1985)57.
11. M.H. Keyder, J. Magn. Magn. Mater. 1 (1990)83.
12. T. Kagotani, D. Fujiwara, S. Sugimoto, K. Inomata, M. Homma, J. Magn. Magn. Mater. e1813 (2004)272.
13. O. Kabo, T. Ido, H. Yokoyama, IEEE Trans. Magn. 1122 (1982)80.
14. W. Zhong, W.P. Ding, N Zhang, J. Magn. Magn. Mater. 196 (1997)168.
15. S.E. Jacobo, C. Domingo-Pascual, R. Rodriguez-Clement, J. Mater. Sci. 1025 (1997)32.
16. K. Haneda, C. Miyakawa, H. Kojima, J. Am. Ceram. Soc. 354 (1974)57.
17. A. Ataie, M.R. Piramoon, I.R. Harris, C.B. Ponton, J. Mater. Sci. 5600 (1995)30.
18. H. Kumazawa, Y. Maedaand, E. Sada, J. Mater. Sci. Lett. 68 (1995)14.
19. V. Pillai, P. Kumar, D.O. Shah, J. Magn. Magn. Mater. 299 (1992)116.
20. J. Smith, H.P.J Wijn, Ferrites, Philips' Technical Library, Eindhoven, 1959.
21. F.K. Lotgering, P.H.G. Vromans, J. Am. Ceram. Soc. 60(1977)416.
22. K. Jisheng, L. Huaixian, D. Youwei, J .Magn. Magn. Mater. 31(1983)801.
23. D. Makovec, A. Kosak, A. Znidarsic, V. Drofenik, J. Magn. Magn. Mater. 289(2005)32.
24. A. Joy, S.K. Date, J. Magn. Magn. Mater. 29(2000)218.
25. J.C. Maxwell, Electricity and Magnetism (Oxford University Press, London, 1973.
26. H.F. Yu, K.C. Huang, J. Magn. Magn. Mater. 260(2003)455.
27. Q. Song, Z. Zhang, J. Am. Chem. Soc. 126(2004)6164.
28. E.C. Stoner, E .Wohlfarth, P Philos, Trans. Royal. Soc. London A240 (1948)599.
29. R. Heikes, D. Johnson, J Chem Phys, 26(1957)58.
30. L. Radhapiyari, Phanjoubam, S. N. K. Sharma, C. Prakash, Mater Lett, 44 (2000)65.
31. C. G. Koops, Phys Rev, 83 (1951)121.
32. M. A. EL Haiti M, J Magn Magn Mater,193 (2005)263.
33. N. Rezleseu, E. Rezleseu, Physics Status Solid, 23(1974)575.
34. K. Iwauchi, Japanese Journal of Applied Physics, 23(1974)575.